

Composition of the Synaptic PSD-95 Complex*[§]

Ayşe Dosemeci‡, Anthony J. Makusky§, Ewa Jankowska-Stephens§, Xiaoyu Yang§, Douglas J. Slotta§, and Sanford P. Markey§¶

Postsynaptic density protein 95 (PSD-95), a specialized scaffold protein with multiple protein interaction domains, forms the backbone of an extensive postsynaptic protein complex that organizes receptors and signal transduction molecules at the synaptic contact zone. Large, detergent-insoluble PSD-95-based postsynaptic complexes can be affinity-purified from conventional PSD fractions using magnetic beads coated with a PSD-95 antibody. In the present study purified PSD-95 complexes were analyzed by LC/MS/MS. A semiquantitative measure of the relative abundances of proteins in the purified PSD-95 complexes and the parent PSD fraction was estimated based on the cumulative ion current intensities of corresponding peptides. The affinity-purified preparation was largely depleted of presynaptic proteins, spectrin, intermediate filaments, and other contaminants prominent in the parent PSD fraction. We identified 525 of the proteins previously reported in parent PSD fractions, but only 288 of these were detected after affinity purification. We discuss 26 proteins that are major components in the PSD-95 complex based upon abundance ranking and affinity co-purification with PSD-95. This subset represents a minimal list of constituent proteins of the PSD-95 complex and includes, in addition to the specialized scaffolds and N-methyl-D-aspartate (NMDA) receptors, an abundance of α -amino-3-hydroxy-5-methyl-4-isoxazolepropionic acid (AMPA) receptors, small G-protein regulators, cell adhesion molecules, and hypothetical proteins. The identification of two Arf regulators, BRAG1 and BRAG2b, as co-purifying components of the complex implies pivotal functions in spine plasticity such as the reorganization of the actin cytoskeleton and insertion and retrieval of proteins to and from the plasma membrane. Another co-purifying protein (Q8BZM2) with two sterile α motif domains may represent a novel structural core element of the PSD. *Molecular & Cellular Proteomics* 6:1749–1760, 2007.

The postsynaptic density (PSD)¹ is a disk-shaped protein complex lining the postsynaptic membrane. In a recent study

its total mass was estimated to be around 1 million kDa (1). The function of this massive protein complex appears to be anchoring and organizing postsynaptic neurotransmitter receptors and corresponding signaling molecules at the active zone. Thus, it is expected that the extent and type of the postsynaptic response to neurotransmitter release will largely depend on the molecular composition and organization of the PSD.

The first tentative identification of PSD components was done in the late 1970s when several laboratories developed the methodology to isolate PSD fractions and started analyzing them by biochemical methods (2, 3). The general strategy, still applied today, was treatment of synaptosomal fractions with detergents that solubilize membranes but leave the PSD relatively intact and subsequent separation of membrane-free PSDs by further centrifugation. Analysis of PSD fractions continued to reveal additional putative PSD components in later years (4) and gained new momentum with the introduction of mass spectrometric techniques (5–14). The development of two-hybrid screens and other methods to determine binding partners of already identified components added important complementary approaches (for a review, see Ref. 15).

The global proteomics analysis of isolated PSDs remains a crucial first step in the elucidation of the molecular structure of the PSD. Indeed the strategy constitutes a relatively simple and convenient way for the identification of hundreds of proteins in a single run: one of the most recent studies identified a total of 1264 proteins (13). Also unlike immunological approaches, the strategy is not based on any *a priori* notion of PSD constituents and therefore can reveal hitherto unsuspected elements. A recent study (16) integrated data from seven proteomics studies (5–9, 17) and other literature on the analysis of PSD fractions. Collins *et al.* (16) report that altogether 1124 proteins were identified in these seven studies. However, 58% of the proteins were detected in only one study, raising the possibility of a high rate of false positives. The authors also compiled a “consensus PSD” list of 467 proteins that were identified in at least two of the studies, thus reducing the probability of false positives linked to individual protocols.

From the ‡Laboratory of Neurobiology, NINDS, National Institutes of Health and §Laboratory of Neurotoxicology, National Institute of Mental Health, Bethesda, Maryland 20892

Received, January 31, 2007, and in revised form, June 15, 2007

Published, MCP Papers in Press, July 9, 2007, DOI 10.1074/mcp.M700040-MCP200

¹ The abbreviations used are: PSD, postsynaptic density; NMDA,

N-methyl-D-aspartate; AMPA, α -amino-3-hydroxy-5-methyl-4-isoxazolepropionic acid; Arf, ADP-ribosylation factor; SAM, sterile α motif; CaMKII, calcium/calmodulin-dependent protein kinase II; EM, electron microscopy; SAPAP, SAP90/PSD-95-associated protein; TARP, transmembrane AMPA receptor regulatory protein; BRAG, brefeldin A-resistant ArfGEF; GEF, guanine nucleotide exchange factor; GAP, GTPase-activating protein.

Although the 467 proteins in the consensus PSD list have a better probability of being genuine PSD components, detection in multiple studies does not necessarily prove that they are. In fact, there seem to be only a handful of proteins that were identified in all seven of the studies (Ref. 16 and Supplemental Tables S2 and S3 in Ref. 16), and this high consensus group includes, in addition to the expected PSD components such as PSD-95, homer, and CaMKII, likely contaminants such as synapsins and intermediate filaments. Moreover because the probability of detection of a protein in a mixture increases with its relative abundance, it is likely that the contaminants in this group are among the most abundant in PSD fractions.

Detection of the same contaminants in all proteomics studies suggests a systemic contamination problem in PSD fractions in general. The most widely applied protocol for the preparation of PSD fractions is the one originally developed by Carlin *et al.* (18) and uses the relatively mild detergent Triton X-100. Because Triton X-100 is mild, it appears to cause minimal loss of protein from the PSD as judged from morphological criteria. On the other hand, many proteins that are present in the synaptosomal fraction but are not part of the PSD also appear to be resistant to Triton X-100. Indeed electron microscopy (EM) analyses of PSD fractions prepared by this method reveal various particulate contaminants including filamentous material and other protein complexes (19, 20). Some of the filamentous materials that are not associated with the PSD have been identified as neurofilaments and spectrin (20).

Altogether these considerations indicate the need for a purer preparation as a basis for the identification of PSD components. The use of a stronger detergent such as *N*-laurylsarcosinate (21) eliminates certain contaminants but also appears to dissociate some genuine PSD elements as well. In addition, certain contaminants such as the so-called "CaMKII clusters" that are resistant to the detergent become enriched in the *N*-laurylsarcosinate-derived PSD fraction (19). On the other hand, because most particulate contaminants in the PSD fraction are membrane-free protein complexes like the PSDs themselves, they are expected to be of the same density as PSDs, excluding the possibility of further fractionation by conventional centrifugation-based techniques.

Affinity-based separation techniques targeting ubiquitous PSD components constitute an orthogonal approach for the isolation of postsynaptic protein complexes, a strategy expected to avoid the problem of detergent-insoluble particulate material contamination prevalent in conventional density-based PSD preparations. Using this approach the isolation of NMDA receptor and PSD-95 complexes from whole cell deoxycholate extracts has been reported (22, 23). However, because these preparations are from detergent-solubilized starting material, isolated complexes tend to be small. Indeed the molecular mass of NMDA receptor complexes was estimated to be around 2000 kDa, which is about 3 orders of magnitude smaller than the whole PSD complex. Thus, the

preparation presumably contains receptor complexes that become dissociated from the bigger PSD complex upon treatment with the relatively strong detergent deoxycholate. In addition, because whole cell extracts are used as starting material, complexes that originate from extrasynaptic/intracellular pools are expected to co-purify with complexes from the PSD. These may include extrasynaptic receptors and transport packages.

We evaluated an affinity-based strategy for the isolation of large PSD-95-containing complexes from the Triton X-100-derived PSD fraction (20). The strategy aims to minimize the contribution from extrasynaptic/intracellular PSD-95 pools by starting with a PSD-enriched fraction from which such non-synaptic complexes have been largely eliminated. Importantly by using magnetic beads coated with a PSD-95 antibody, large, insoluble complexes are separated without the use of additional detergents to solubilize particulates.

Postsynaptic PSD-95 complexes are likely to represent the bulk of the PSD observed by EM in intact cells. Indeed PSD-95 is able to interact with a large number of proteins through its three PDZ domains, an SH3 domain, and a guanylate kinase domain and also can multimerize to form an extended scaffold (for a review, see Ref. 15). Moreover proteins that bind PSD-95 in turn interact with yet other postsynaptic components, thus extending the network. The complexes isolated using PSD-95 antibody-coated magnetic beads resemble *in situ* PSDs (20), suggesting that most if not all of the original components have been retained. These considerations suggested that analysis of the isolated PSD-95 complexes would identify most if not all of the components of the *in situ* PSD.

In the present study, isolated PSD-95 complexes and the parent PSD fraction were analyzed in parallel by liquid chromatography coupled to tandem mass spectrometry. For each fraction, identified proteins were ranked according to cumulative ion current intensities of corresponding peptides as a semiquantitative measure of relative abundance. Comparison of the ranks of proteins in the parent and affinity-purified preparations allowed identification of those that co-purify with PSD-95 and, importantly, those that are likely contaminants.

MATERIALS AND METHODS

Preparation of the PSD Fraction and Isolation of PSD-95 Complex—The PSD fraction was prepared essentially by the method of Carlin *et al.* (18) with modifications as described previously (19). Brains from adult Sprague-Dawley rats were custom collected by Pel Freez Biologicals (Rogers, AR), frozen immediately in liquid nitrogen, and shipped on dry ice. Brains were thawed by a 1-min immersion in isotonic sucrose at 37 °C and dissected on ice to remove white matter, and cerebral cortices were then rapidly homogenized. A synaptosomal fraction was obtained and treated with 0.5% Triton X-100. Detergent-insoluble pellets were collected, and a PSD-enriched fraction was separated by sucrose density centrifugation. This fraction was extracted once more with 0.5% Triton X-100, 75 mM KCl.

Isolation of PSD-95 complexes was as described previously (20) with some modifications. Dynabeads (M-450 coated with goat anti-mouse IgG) were obtained from Dynal (Oslo, Norway) and were fur-

ther coated with a monoclonal PSD-95 antibody (MA1-046; ABR-Affinity BioReagents, Inc., Golden, CO). PSD fraction (200 μg of protein) was resuspended in 10 ml of 2% BSA (of 99% purity to minimize contamination of the preparation by the blocker), 0.01% Tween 20 in phosphate-buffered saline using a probe sonicator. Sonication (3×1 min with ~ 3 min cooling intervals in ice) was done at the lowest power setting (<5 watts) taking care not to warm the samples. Resuspended PSD fraction (200 μg) was incubated with antibody-coated magnetic beads (2×10^8 beads) in a final volume of 10 ml for 2 h at 4 $^{\circ}\text{C}$ with continuous rotation. Unbound material was removed, and the beads were washed three times with 2% BSA, 0.01% Tween 20 in phosphate-buffered saline and five times with 0.01% Tween 20 in phosphate-buffered saline for a total of ~ 3 h.

Fractionation and Mass Spectrometric Analysis of Preparations—The parent PSD fraction or washed beads with attached complexes were treated with SDS-containing electrophoresis sample buffer and were incubated in boiling water for 5 min. Solubilized affinity-purified samples corresponding to the yield from ~ 100 μg of starting PSD fraction were loaded onto individual gel lanes. Gels were stained with Coomassie Brilliant Blue to visualize bands for imaging and then sectioned from the top of the gel to the bottom in 2-mm increments, and the pieces were placed in clean Eppendorf tubes. In-gel tryptic digestion was performed after two washes with 50% acetonitrile in 100 mM ammonium bicarbonate, and dehydration of gel slices was performed with the addition of 100% acetonitrile. Disulfides were reduced with 45 mM dithiothreitol in 50 mM ammonium bicarbonate and alkylated with 100 mM iodoacetamide in 50 mM ammonium bicarbonate. Gel pieces were again dehydrated with 100% acetonitrile. Trypsin (260 ng/gel piece) was added and incubated overnight at room temperature. Peptides were extracted from the gel pieces by subsequent additions of 30% acetonitrile in 0.1% TFA and 80% acetonitrile in 0.1% TFA. Samples were dried, redissolved in 0.1% formic acid, and injected into a Shimadzu HPLC system coupled to a Thermo Finnigan LCQ Classic instrument (24). HPLC separation was performed on a New Objectives Pico-frit column filled with BetaBasic C₁₈. A linear gradient was developed from 10 to 60% B (A, 5% acetonitrile, 95% aqueous 0.1% formic acid; B, 80% acetonitrile, 20% aqueous 0.1% formic acid) at a rate of 1.5%/min. Data were collected continuously for 60 min, selecting the three most intense ions (exceeding 3×10^6 intensity units) in an MS survey scan to subsequent MS/MS analyses using collisionally induced dissociation. Selected precursors were analyzed for two MS/MS cycles and then excluded for redundant analyses for a 90-s interval. Thermo Finnigan Excalibur 2.0 utility extract_msn was used to retrieve peak lists without any added smoothing or signal to noise ratio criteria. The recorded MS/MS files were searched with the Mascot search engine 2.1.04 (Matrix Sciences, London, UK) against the Swiss-Prot database (Sp_Trembl_122406.fas) with the limitation of mammalian species for protein database records; precursor ion mass tolerance, 2.0; fragment ion mass tolerance, 0.8; methionine oxidation and carbamidomethylation of cysteine allowed; and trypsin specificity with one missed cleavage allowed.

Mascot-assigned peptides with Ion Score exceeding their Identity Score were then grouped using the software tool DBParser 2.0 (25), and reports were generated for each lane from the concatenated Mascot files. DBParser 2.0 was also used to compare data from multiple lanes at both the peptide and protein levels. DBParser 3.0 was used to extract ion current intensity values for peptides with Mascot Ion Scores greater than Identity Scores (DBParser 3.0 is further described in Supplement 1).

RESULTS

PSD-95 complexes were affinity-purified from the conventional PSD fraction using magnetic beads coated with an

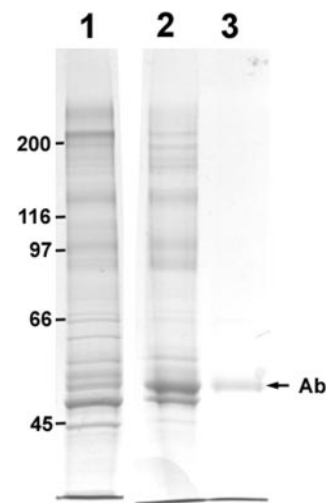


FIG. 1. Coomassie blue-stained SDS gel (7.5% acrylamide). Lane 1, parent PSD fraction; Lane 2, PSD-95 complex affinity-purified with antibody-coated magnetic beads; Lane 3, control, eluant when beads coated with secondary antibody only were incubated with PSD fraction. The position of the antibody (Ab) heavy chain is shown with an arrow. Lane 2 contains PSD-95 antibody and secondary antibody, whereas Lane 3 contains secondary antibody only. Positions of molecular mass standards (in kDa) are indicated on the left.

antibody against the core PSD protein PSD-95. Parent and affinity-purified samples were separated by one-dimensional SDS gel electrophoresis and analyzed in parallel. The control sample (Fig. 1, Lane 3) shows no visible band except the secondary antibody used to coat the magnetic beads, indicating the absence of nonspecific binding. The protein profiles of the parent PSD fraction (Fig. 1, Lane 1) and of the affinity-purified PSD-95 complex (Fig. 1, Lane 2) are different, indicating removal of several proteins during purification.

Gel lanes in their entirety were cut into 40 fractions, digested with trypsin, and analyzed by LC/MS/MS. The resulting mass spectra were assigned probable peptide sequences using the Mascot search engine (Matrix Sciences). For these studies, the Swiss-Prot mammalian protein reference library was selected, and peptides with Mascot Ion Scores exceeding their Identity Scores were analyzed and grouped using DBParser 2.0. This software applies parsimony analysis to reduce the thousands of identified peptides to a minimal protein list (25). Only proteins from the minimal protein list were considered for further evaluation (Tables I–IV). The results from the two preparations include protein assignments from homologous mammalian proteins other than rat as indicated in the tables of results.

Altogether three sets of samples were analyzed, corresponding to two independent parent and affinity-purified preparations. The concatenated parent (from 133 LC/MS/MS runs) and affinity-purified (125 LC/MS/MS runs) files correspond to summed and integrated analyses. Identified proteins were ranked according to summed ion current intensities of their constituent peptides as a relative abundance index.

Composition of the Synaptic PSD-95 Complex

TABLE I

50 top ranking of proteins in the affinity-purified PSD-95 complex

Proteins are ranked in descending order of summed ion current intensity. For complete peptide sequences and statistical confidence scores, refer to Supplemental Table 1.

Affinity purification rank	Parent rank	Protein (family) common name	UniProt KB/Swiss-Prot entry	Unique peptides
1	1	CaMKII	KCC2A_RAT	9
2	4	PSD-95	DLG4_RAT	25
3	3	β -Tubulin	TBB5_RAT	16
4	7	SynGAP	SYGP1_RAT	24
5	2	α -Tubulin	Q5XIF6_RAT	10
6	10	PSD-93	DLG2_RAT	16
7	27	GluR2	GRIA2_RAT	24
8	6	Actin	ACTB_RAT	6
9	23	Shank3	SHAN3_RAT	25
10	22	BRAG1 (KIAA0522)	O60275_HUMAN	20
11	17	Hypothetical	Q8BZM2_MOUSE	9
12	48	GluR3	GRIA3_RAT	13
13	35	Homer	HOME1_RAT	10
14	19	Shank1	SHAN1_RAT	24
15	26	Shank2	SHAN2_RAT	18
16	14	IRSp53	BAIP2_RAT	12
17	49	BRAG2b	Q6DN90_HUMAN	4
18	61	GluR1	GRIA1_RAT	7
19	24	Densin 180	LRRC7_RAT	13
20	13	α -Catenin	Q5R416_PONPY	13
21	20	Glutamine synthetase	GLNA_RAT	7
22	65	SAPAP4	DLGP4_RAT	4
23	44	SAPAP1	DLGP1_RAT	8
24	29	ADP/ATP translocase	ADT1_RAT	6
25	47	SAPAP3	DLGP3_MOUSE	8
26	45	NMDAR2B	NMDE2_RAT	13
27	16	Myosin 10	MYH10_RAT	13
28	66	SAPAP2	DLGP2_RAT	6
29	32	PP1	PP1A_RAT	7
30	76	Neurologin	NLGN3_RAT	7
31	87	Hypothetical (FAM81A)	Q8TBF8_HUMAN	5
32	>93	GLUR4	GRIA4_MOUSE	6
33	84	Cylindromatosis	Q66H62_RAT	8
34	30	PKC- γ	KPCG_RAT	5
35	12	SNIP	SNIP_RAT	6
36	9	Plectin	PLEC1_RAT	23
37	25	Heat shock cognate 71	HSP7C_RAT	8
38	62	NMDAR2A	O08948_RAT	8
39	37	SAP97	DLG1_HUMAN	4
40	36	SAP102	DLG3_RAT	5
41	92	Leu-rich repeat . . .	LRTM1_HUMAN	2
42	59	Hypothetical (FLJ35778)	Q8NA73_HUMAN	3
43	15	VDAC1	VDAC1_RAT	7
44	38	Citron	Q9QX19_RAT	6
45	60	NMDAR1	Q62648_RAT	5
46	58	TARP	CCG8_RAT	2
47	18	α -Actinin	Q6GMN8_RAT	7
48	28	G3P	G3P_RAT	6
49	41	Kalirin	HAPIP_RAT	12
50	69	CPG2 protein	Q63128_RAT	5

DBParser 3.0 extracts retention time and peak intensity from raw data based on the precursor mass identified by the search engine as described previously for ion trap LC/MS/MS data (26). The corresponding maximum intensity, peak area, and number of scans for each identified peptide were then

calculated from respective selected ion chromatograms recorded during the survey scan cycle (see Supplement 1 for DBParser 3.0 details).

Known contaminants, originating from sources other than brain tissue, including immunoglobulins (antibodies used for

TABLE II
50 top ranking of proteins in the conventional (parent) PSD fraction

Proteins are ranked in descending order of summed ion current intensity. For complete peptide sequences and statistical confidence scores, refer to Supplemental Table 2.

Parent rank	Affinity purification rank	Protein (family) common name	UniPost KB/ Swiss-Prot entry	Unique peptides
1	1	CaMKII	KCC2A_RAT	11
2	5	α -Tubulin	Q5XIF6_RAT	13
3	3	β -Tubulin	TBB5_RAT	15
4	2	PSD-95	DLG4_RAT	24
5	59	α -Spectrin	SPTA2_RAT	52
6	8	Actin	ACTB_RAT	7
7	4	SynGAP	SYGP1_RAT	27
8	69	Bassoon	BSN_RAT	38
9	36	Plectin	PLEC1_RAT	60
10	6	PSD-93	DLG2_RAT	15
11	67	α -Internexin	AINX_RAT	11
12	35	SNIP	SNIP_RAT	18
13	20	α -Catenin	Q5R416_PONPY	19
14	16	IRSp53	BAIP2_RAT	14
15	43	VDAC1	VDAC1_RAT	13
16	27	Myosin 10	MYH10_RAT	22
17	11	Hypothetical (SAM/PTB)	Q8BZM2_MOUSE	11
18	47	α -Actinin	Q6GMN8_RAT	28
19	14	Shank1	SHAN1_RAT	17
20	21	Glutamine synthetase	GLNA_RAT	7
21	74	Synapsin 2	SYN2_RAT	16
22	10	BRAG1 (KIAA0522)	O60275_HUMAN	14
23	9	Shank3	SHAN3_RAT	14
24	19	Densin 180	LRRC7_RAT	15
25	37	Heat shock cognate 71	HSP7C_RAT	12
26	15	Shank2	SHAN2_RAT	11
27	7	GluR2	GRIA2_RAT	9
28	48	G3P	G3P_RAT	7
29	24	ADP/ATP translocase	ADT1_RAT	8
30	34	PKC- γ	KPCG_RAT	8
31	71	ERC protein 2	ERC2_RAT	12
32	29	PP1	PP1A_RAT	10
33	52	β -Catenin	CTNB1_HUMAN	11
34	73	VDAC2	VDAC2_RAT	8
35	13	Homer	HOME1_RAT	9
36	40	SAP102	DLG3_RAT	11
37	39	SAP97	DLG1_HUMAN	3
38	44	Citron	Q9QX19_RAT	7
39	60	GAPDH	Q8K417_SIGHI	4
40	56	ArgBP2	O35413_RAT	8
41	49	Kalirin	HAIIP_RAT	11
42	63	N-cadherin	CADH2_RAT	6
43	62	VDAC3	Q6GSZ1_RAT	6
44	23	SAPAP1	DLGP1_RAT	8
45	26	NMDAR2B	NMDE2_RAT	7
46	61	Fructose bisphosphate aldolase	ALDOA_RABIT	2
47	25	SAPAP3	DLGP3_MOUSE	10
48	12	GluR3	GRIA3_RAT	6
49	17	BRAG2b	Q6DN90_HUMAN	6
50	66	Mitochondrial glutamate carrier	GHC1_MOUSE	6

affinity purification), serum albumin (blocker), trypsinogen, and human keratin were deleted from the lists. The lists were condensed further by reporting certain related proteins with multiple isoforms as a single family. Families of proteins are represented by their most abundant member. For example,

although α -, β -, δ -, and γ -isoforms of CaMKII were identified, CaMKII is reported by a single entry corresponding to its most abundant α -isoform.

Tables I and II list the highest ranking 50 proteins from the simplified lists corresponding to affinity-purified and parent

TABLE III
Proteins co-purifying with PSD-95

Proteins from Table I (50 top ranking proteins in the affinity-purified preparation) with a normalized ion current intensity ratio greater than 0.5 are included.

Protein (family) name	UniProt KB/ Swiss-Prot entry	Change in rank (parent/affinity-purified)	Normalized ion current intensity ratio (purified/parent)
Glutamate receptors			
GluR2 (AMPA)	GRIA2_RAT	27/7	>1
GluR3 (AMPA)	GRIA3_RAT	48/12	>1
GluR1 (AMPA)	GRIA1_RAT	61/18	>1
GluR4 (AMPA)	GRIA4_RAT	>93/32	>1
NMDAR2B	NMDE2_RAT	45/26	0.55
NMDAR2A	O08948_RAT	62/38	>1
NMDAR1	Q62648_RAT	60/45	0.74
Scaffolds			
PSD-95	DLG4_RAT	4/2	1.00
PSD-93	DLG2_RAT	10/6	0.67
Shank3	SHAN3_RAT	23/9	>1
Hypothetical (SAM/PTB)	Q8BZM2_MOUSE	17/11	0.62
Homer	HOME1_RAT	35/13	>1
Shank2	SHAN2_RAT	26/15	0.75
SAPAP4	DLGP4_RAT	65/22	>1
SAPAP1	DLGP1_RAT	44/23	0.59
SAPAP2	DLGP2_RAT	66/28	>1
G-protein regulators			
SynGAP	SYGP1_RAT	7/4	0.64
BRAG1 (KIAA0522)	O60275_HUMAN	22/10	>1
BRAG2b	Q6DN90_HUMAN	49/17	>1
Other			
Neuroigin	NLGN3_RAT	76/30	>1
Hypothetical (FAM81A)	Q8TBF8_HUMAN	87/31	>1
Cylindromatosis	Q66H62_RAT	84/33	>1
Leu-rich repeat . . .	LRTM1_HUMAN	92/41	>1
Hypothetical (FLJ35778)	Q8NA73_HUMAN	59/42	0.73
TARP (γ 8)	CCG8_RAT	58/46	0.62
CPG2 protein	Q63128_RAT	69/50	0.95

samples, respectively. The tables include only those proteins detected in both fractions and thus allow a fair comparison by rank order. The proteins are listed in descending rank order (highest ion current intensity at the top). Only proteins identified by two or more peptides were included in determining rank order. The second columns in Tables I and II show the rank of the same protein in the other group. Although a number of factors in addition to the abundance of a protein may influence the ion current intensity, these other factors are expected to remain the same for the two fractions so that a change in rank order may be used as an indication of a change in relative abundance. The last columns in Tables I and II indicate the number of peptides identified by MS/MS exclusively associated with the assigned proteins and used for intensity determinations. There is no direct correlation between the number of peptides and total ion current intensity as the number of peptides detectable is a function of both the number of possible tryptic products compatible with mass spectrometric detection and their relative abundance.

As a measure of co-purification with PSD-95, the ratios of normalized ion current intensities in the affinity-purified group

over that in the parent group were calculated for individual proteins (Tables III and IV, last columns). To compensate for variable total protein contents of samples applied to gels, ion current intensities for individual proteins were normalized with respect to the ion current intensity for PSD-95 in the same sample. For certain proteins, the ratios of normalized ion current intensities were greater than 1 implying that immunofluorescence capture of PSD-95 resulted in the capture of additional specific proteins with higher efficiency than the targeted PSD-95. However, this phenomenon is more likely the result of signal to noise ratio differences between the parent and affinity-purified protein mixtures. Chemical noise from peptides from contaminant proteins masks co-eluting peptides from constitutive proteins present in the parent mixture. Thus, peptides from some proteins are observable only after affinity purification. Comparable amounts of PSD-95 (DLG4) were analyzed in each preparation (24 peptides observed in the parent preparation, summed intensity: 7×10^9 ; 25 peptides in the affinity-purified, summed intensity: 9×10^9). After removal of interfering peptides from contaminants, signals from peptides from the constituents of the PSD-95 complex were

TABLE IV
 Proteins greatly reduced/depleted in the affinity-purified PSD-95 complex

Proteins from Table II with a normalized ion current intensity ratio of 0.1 or smaller were included. Certain proteins (not applicable, NA) were abundant in the parent fraction with intensities that would rank them in the top 50 proteins but were not detected after affinity purification. ID, identity; int., intensity; SNIP, SNAP-25-interacting protein.

Protein (family) name	UniProt KB/ Swiss-Prot entry	Change in rank (parent/purified)	Normalized ion current intensity ratio (purified/parent)
Presynaptic proteins			
Bassoon	BSN_RAT	8/69	0.01
SNIP	SNIP_RAT	12/35	0.06
Synapsin 2	SYN2_RAT	21/74	0.02
ERC protein 2	ERC2_RAT	31/71	0.04
Synapsin 1	SYN1_RAT	NA ^a	0.00
Piccolo	PCLO_RAT	NA ^a	0.00
RIM	RIMS_RAT	NA ^a	0.00
Cytoskeletal elements			
α -Spectrin	SPTA2_RAT	5/59	0.01
Plectin	PLEC1_RAT	9/36	0.04
α -Internexin	AINX_RAT	11/67	0.01
β -Spectrin	SPTN2_RAT	NA ^a	0.00
Neurofilament-L	NFL_RAT	NA ^a	0.00
Neurofilament-M	NFM_RAT	NA ^a	0.00
Different organelle/cell type			
VDAC1 (mitochondrial)	VDAC1_RAT	15/43	0.06
VDAC2 (mitochondrial)	VDAC2_RAT	34/73	0.04
Myelin basic protein	MBP_RAT	NA ^a	0.00
Ribosomal proteins	RLA0_RAT	NA ^a	0.00
Other			
α -Actinin	Q6GMN8_RAT	18/47	0.06
Synaptopodin	SYNPO_RAT	NA ^a	0.02
β -Catenin	CTNB1_HUMAN	33/52	0.09
N-cadherin	CADH2_RAT	42/63	0.09

^a Proteins identified with two or more peptides in parent fraction only.

detected more readily. For example, GluR1 (GRIA1_RAT) was characterized by three peptides in 113 MS scans (summed intensity, 2×10^8) in the parent mixture and by seven peptides in 274 MS scans (9×10^8) after affinity purification. The semiquantitative nature of this method assesses relative ranking but cannot be used to infer stoichiometry.

Table III lists those proteins that co-purify with PSD-95 by two criteria presented in the last two columns: change in rank order and normalized ion current intensity ratio (purified/parent). Only the 50 top ranking proteins from the affinity-purified group (Table I) were considered, and the cutoff point for inclusion in the list was a normalized ion current intensity ratio of 0.5. It can be observed that 26 of the 50 top ranking proteins met these criteria and also demonstrated a substantial decrease in rank order (Table III). The 26 proteins shown in Table III are relatively abundant components that are substantially co-purified with PSD-95 and thus most likely represent a minimal list of constitutive PSD-95 complex proteins.

Table IV lists those proteins that are depleted or greatly reduced in the affinity-purified sample with the same indexes as in Table III. For this list, those proteins from Table II (top ranking proteins from the parent group) with normalized ion current intensity ratios of parent/purified below 0.1 were selected. Also five additional top ranking proteins that were

detected in the parent group only were included. Of the 21 proteins that show significant reduction/depletion in purified samples, seven are presynaptic elements, and six are cytoskeletal elements.

DISCUSSION

The molecular architecture of the PSD-95 complex is less readily definable than that of the synaptic vesicle as elegantly described by Takamori *et al.* (27). In the course of that work, the value of immunoaffinity-assisted isolation was recognized in the proteomics analyses of light and heavy synaptic vesicles by Morciano *et al.* (28). Both heavy and light sucrose density gradient-separated vesicles contain many proteins in common, but the sedimented heavy fraction was contaminated with PSD proteins until separated with anti-SV2 monoclonal antibody-coated magnetic beads. The heavy fraction was then found to consist of synaptic vesicles docked to presynapse plasma membranes but was free of PSD proteins (28). In an analogous manner, we sought to demonstrate that the immunoaffinity-assisted isolation of the PSD-95 complex developed by Vinade *et al.* (20) provides an isolate more relevant to defining the composition of the PSD-95 complex because it is substantially freer from co-sedimenting components than attainable by sucrose density centrifugation alone.

TABLE V
Comparison of proteins observed with literature data

Bold values are data from the present study. For complete protein information, peptide sequences, and statistical confidence scores, refer to Supplemental Tables 3–6.

Confidence ^a	Proteins reported ^b	Parent preparation	Affinity purification
8	10	10	8
7	13	13	12
6	15	15	12
5	34	30	25
4	62	56	31
3	135	91	50
2	198	112	45
1	657	192	101
Totals	1124	525	288

^a Consensus number of studies reporting identification of the same set of proteins.

^b Number of proteins in the set (Collins *et al.* (16)).

Because the identification of proteins in the PSD fraction has been the subject of multiple reports, we have reconciled our findings with those of others. Repeated observation of the same proteins by multiple investigators adds certainty to the identified constituents of the PSD fraction. Collins *et al.* (16) collected and correlated reports from seven laboratories and the literature to assemble a non-redundant set of 1124 accession numbers of proteins. The task of comparing protein identifications is not possible without access to either the original tandem mass spectrometry data or the peptide sequences ascribed to that data. Protein accession numbers and entry names change when protein databases are curated so that differences in published lists of proteins are sometimes due to differences in the versions of the protein reference libraries used for sequence assignment. Consequently we compiled protein sequence fasta files for the entries tabulated by Collins *et al.* (16) and used these reference sublibraries for Mascot to re-search and identify proteins. The use of the Collins *et al.* (16) sublibrary (kindly provided by the authors) ensures that peptide sequences recognized can be mapped to the same protein names, eliminating ambiguity of naming conventions or isoform selection. Table V summarizes these results parsed and analyzed using MassSieve software.²

The proteins identified in our parent preparation are consistent with those reported by others. Of 134 proteins observed by four or more laboratories, we identified peptides from 124 (92%). Of greater importance are differences observed after affinity purification: only 88 (57%) of the 134 proteins observed by four or more laboratories were observed after affinity purification presumably due to removal of contaminating proteins.

In the present study large, affinity-purified PSD-95 com-

² D. Slotta, M. A. McFarland, and S. P. Markey, manuscript in preparation.

plexes derived from the synapse were analyzed, and on the basis of rank order changes with respect to the parent PSD fraction, a subset of the identified proteins were selected as likely to be consistent, integral components of the complex. It should be noted that the 26 proteins included in Table III constitute a minimal list of relatively abundant constituents of the PSD-95 complex. The PSD-95 complex undoubtedly includes additional components. Indeed a much larger number of proteins than those listed in Table III have been identified in the affinity-purified preparation (see Table V and supplemental tables for a complete list of proteins and constituent identified peptides), and many of these appear to be more prominent than in the parent PSD fraction. However, we have chosen to apply stringent criteria (two or more peptides within the top 50 rank order by intensity and normalized ion current ratios greater than 0.5 relative to PSD-95) that would select only for the relatively abundant proteins that co-purify with PSD-95.

A minimal list of constituent proteins of the synaptic PSD-95 complex (Table III) includes specialized PSD scaffolds with multiple protein interaction sites and receptors as well as several proteins likely to be involved in aspects of spine structure and dynamics such as trafficking of receptors, actin dynamics, and cell adhesion. On the other hand, many of the proteins that are greatly reduced or eliminated upon affinity purification are presynaptic or extrasynaptic in origin (Table IV). Effective removal of these known contaminants attests to the success of the affinity-based strategy and establishes the preparation as a good base for the elucidation of the composition of the PSD complex.

Electron microscopy of the affinity-purified preparation shows many particulate structures that look like PSDs (20), suggesting that the isolated PSD-95 complex retains the bulk of the proteins that make up the *in situ* PSD. However, there are a few proteins, including N-cadherin, catenins, and α -actinin, that have been observed at the contact zone by immuno-EM (29–31) but whose levels decrease with respect to the parent PSD fraction upon affinity purification. This could be due to the dissociation of some loosely bound components during purification as well as the existence of physically separate complexes that co-localize *in situ* with the PSD-95 complex. It is interesting to note that all the above mentioned proteins are associated (either directly or indirectly) with the actin cytoskeleton and may be linked to the PSD-95 complex through actin. Partial disassembly of the actin during the purification protocol may have caused their release. Thus, the affinity-purified preparation appears to include the majority but not all of the components of the *in situ* PSD.

Two measures for affinity co-purification (change in rank order and ratio of normalized ion current intensities) were used to identify integral elements of the PSD-95 complex. The 26 proteins in Table III are thus likely to represent a subset of constituent elements. As discussed below, some of the proteins in the list are expected components of the PSD-95

complex such as specialized PSD scaffolds and NMDA receptors, whereas the involvement of some of the other identified proteins had been somewhat controversial. Definitive stoichiometry of constitutive PSD-95 complex proteins will require either orthogonal techniques such as quantitative Western blotting or stable isotope mass spectrometric standards, and this study refines the list of proteins that should be targeted as well as identifies their proteotypic peptides for synthesis of labeled standards. Most interestingly, the list spotlights certain proteins that had not been generally acknowledged up to now as part of the PSD-95 complex. We discuss below particular proteins in functional groups.

Scaffolds—Most specialized PSD scaffolds are identified as constituents of the PSD-95 complex. Co-purification of PSD-93 with PSD-95, two homologous proteins, each with a guanylate kinase, an SH3, and three PDZ domains (for a review, see Ref. 15), argues against their differential localization in different synapses and indicates that they are part of the same complex. In addition, SAPAPs (SAP90/PSD-95-associated proteins) that bind directly to PSD-95, Shanks that bind to SAPAPs, and homer that binds to Shanks (for a review, see Ref. 15) all co-purify with PSD-95 suggesting that the entire PSD scaffold is preserved in the purified complex.

Shank3, together with PSD-95 and PSD-93, is among the 10 top ranking proteins in the purified fraction. Shanks are thought to multimerize through association of their sterile α motif (SAM) domains (32). Indeed SAM domains that typically spread over ~70 residues have been described to homo- and hetero-oligomerize (for a review, see Ref. 33). A recent report (34) described large sheets made of stacked helical fibers being formed by the SAM domains of Shank3, which, they suggest, may constitute a core platform for the PSD organization. The present analysis identifies a hypothetical protein (Q8BZM2) with two SAM domains as a constituent of the PSD-95 complex. In analogy to other SAM-containing proteins, this protein is expected to homo- and hetero-oligomerize and thus participate in the formation of the PSD scaffold.

Adhesion Molecules—In contrast to cadherin/catenin, another group of cell adhesion molecules, neuroligins, are identified as constituents of the PSD-95 complex. This finding is in agreement with reports on direct binding of the two proteins (35). In addition, the present analysis reveals the presence of yet another putative adhesion molecule, LRTM1, of the leucine-rich repeat transmembrane protein family in the PSD-95 complex (36).

Cytoskeletal Elements—Cytoskeletal elements make up a major proportion of the proteins in the conventional PSD fraction and were observed to be enriched in the PSD fraction compared with the synaptosome fraction (10). However, with the exception of actin and tubulin most cytoskeletal proteins are substantially reduced/depleted in the affinity-purified PSD-95 complex. Actin constitutes the main cytoskeleton of the dendritic spine and interacts with the PSD *in situ* (37). The present data, demonstrating a slight tendency for actin to

co-purify with PSD-95, is in agreement with the notion that actin is an integral element of the PSD. Another cytoskeletal protein, tubulin, also appears to be present in large quantities in the affinity-purified fraction. This is somewhat surprising because microtubules are rarely observed near the PSD of mature spines. One explanation may be that tubulin is attached to the PSD either in monomeric or a different polymeric form; for example, it has been proposed that NMDA receptors have a preferential affinity for soluble forms of tubulin (for a review, see Ref. 38). On the other hand immun-EM studies do not support the presence of large quantities of tubulin at the *in situ* PSD.³ Thus, the possibility remains that at least part of the detected tubulin becomes associated with the PSD-95 complex postmortem when large quantities of depolymerized tubulin become available during homogenization.

In contrast to actin and tubulin, other cytoskeletal elements such as spectrins and intermediate filaments that are prominent in conventional PSD fractions (5, 9, 10) are virtually eliminated upon affinity purification. The removal of spectrin and intermediate filaments suggests that these proteins are not components of the PSD, consistent with the observation of non-associated spectrin filaments and neurofilaments in the parent PSD preparation (20).

Glutamate Receptors and Related Molecules—Glutamate receptors of both NMDA and AMPA types appear to be prominent components of the PSD-95 complex. Our previous work demonstrated by Western immunoblotting the presence of AMPA-type glutamate receptors in the affinity-purified preparation (20). Comparative analysis of the parent and purified fractions in the present study shows that AMPA receptors co-purify with PSD-95. Earlier reports had indicated that NMDA receptor complexes isolated from detergent extracts do not contain AMPA-type receptors (22, 23), an observation that led the authors to conclude that AMPA receptors at the PSD are physically separate from the PSD-95 complex. It is possible that these small NMDA complexes (2000 kDa as compared with 1 million kDa for the PSD) are subcomplexes dissociated from the PSD by the relatively strong detergent (deoxycholate) used. Alternatively they may represent a distinct group of receptors of either synaptic or extrasynaptic origin.

Our observation that AMPA-type receptors are an integral part of the PSD-95 complex is in agreement with accumulated evidence on the regulation of synaptic AMPA receptor levels by PSD-95 (39–42). On the other hand, because direct binding of AMPA receptors to PSD-95 has not been demonstrated, an indirect association through at least one bridging molecule has to be assumed. SAP97 has been detected by Western immunoblotting to be present in affinity-purified complexes (20), but this protein would be able to anchor only those receptors that contain GluR1 subunits. Also the present

³ J.-H. Tao-Cheng, personal communication.

semiquantitative analysis indicates that SAP97 is not particularly enriched in the PSD-95 complex, whereas GluR1 is. A good candidate for bridging all types of AMPA receptors to the core PSD complex is the TARP (Stargazin) family of proteins, which are reported to bind very strongly to AMPA receptors and also to PSD-95 (43). Our results identify TARP γ 8 (CCG8_RAT) as a component of the PSD-95 complex. However, at this stage it is not clear whether the amount of TARP found in the PSD-95 complex is sufficient to support the binding of all AMPA receptors, at least one TARP per five AMPA receptor subunits. Future quantitative studies that assess stoichiometric relationships would clarify that point.

CPG2, a protein that has been proposed to be involved in the constitutive internalization of NMDA- and AMPA-type glutamate receptors and in the activity-induced internalization of AMPA receptors (44) is also a component of the PSD-95 complex. Immuno-EM studies demonstrated that the protein is located laterally and underneath the cytosolic side of the PSD (44). These results together with our data indicating physical attachment of the protein to the PSD-95 complex suggest that CPG2 may be associated as an appendage to the PSD rather than being integrated within the core structure.

CaMKII—The Ca^{2+} -regulated protein kinase CaMKII appears to be the major protein in the PSD-95 complex as judged by its abundance ranking and relative band intensity in Coomassie-stained gels. We had previously demonstrated that part of the CaMKII present in conventional PSD preparations is contributed by contaminating CaMKII clusters, spherical structures \sim 100 nm in diameter (19). Thus, it is remarkable that even after the elimination of these CaMKII clusters in affinity-purified samples CaMKII still remains the most abundant protein. However, it should be noted that this may not hold true for *in situ* PSD-95 complexes at inactive synapses. Indeed the amount of CaMKII associated with the PSD is regulated by synaptic activity. Previous immuno-EM studies have shown that excitatory and ischemia-like conditions cause severalfold increases in CaMKII labeling of the PSD (19, 45, 46). Ischemia-like conditions that prevail during the dissection of brain tissue likewise cause an increase in the CaMKII content of PSD fractions (47). Thus, for the case of CaMKII and certain other variable/transient components of the postsynaptic complex such as GluR1, the abundance is likely to be determined by factors such as the level of neuronal activity and anesthesia prior to sacrifice as well as by post-mortem handling.

Small G-protein Regulators—A substrate for CaMKII, the synaptic Ras GTPase-activating protein SynGAP (48) is also among the abundant proteins in the purified PSD-95 complexes. SynGAP can directly bind to PSD-95 (49). Parallel analysis of parent and affinity-purified fractions highlighted the presence of two additional small G-protein regulators of the brefeldin A-resistant ArfGEF (BRAG) family in the PSD-95 complex. One of these (KIAA0522, O60275_HUMAN, IQEC2_HUMAN, gi|62666747|ref|XP_228841.3) has been

classified as BRAG1 (50). A recent study (51) published during the preparation of this manuscript identifies an error in the sequence of KIAA0522 and demonstrates *in situ* co-localization of BRAG1 and PSD-95. BRAG1 is enriched in the PSD-95 fraction compared with the synaptosome fraction (10, 51). BRAG1 is a 190-kDa protein with a calmodulin binding IQ domain and a sec7 domain, a \sim 200-amino acid signature sequence for ArfGEFs that confers guanine nucleotide exchange activity. BRAG1 has been shown to regulate Arf1 (51), and from the sequence similarity, it is probable that it also acts on Arf6 (49).

Surprisingly another member of the same family, BRAG2b (Q6DN90_HUMAN, IQEC1_HUMAN), is also identified in the PSD-95 complex. BRAG1 and BRAG2b are distinguishable proteins and were identified by two entirely different sets of peptides with no overlapping assignments. BRAG2b is a splice isoform of a previously identified ArfGEF (Arf-GEP100 (52) and has been shown to regulate Arf6 (53). Another ArfGEF called SynArfGEF (Q76M68) has recently been reported by Inaba *et al.* (54) to be enriched in the PSD fraction and is suggested to act on Arf1. SynArfGEF was not observed in this study and differs from both BRAG1 and BRAG2b (63 and 48% homology, respectively).

Arfs are from the Ras family of small G-proteins that regulate membrane trafficking and the actin cytoskeleton. Different types of Arfs appear to be targeted to different subcellular locations (for reviews, see Refs. 55 and 56): Arf1 is preferentially targeted to the Golgi, whereas Arf6 is localized at the plasma membrane and to some extent on endosomes (for reviews, see Refs. 56 and 57). Interestingly Arf6 has been implicated in the insertion of and retrieval of membrane proteins at defined sites as well as in the reorganization of the actin cytoskeleton that results in various forms of membrane remodeling (for a review, see Ref. 57). Considering that synaptic strength is largely regulated by the insertion and retrieval of receptors to and from the postsynaptic contact zone and that actin is a constituent of the cytoskeleton at the spine, the potential relevance of Arf6 to spine structure and function becomes obvious. In fact, two recent studies (58, 59) already reported involvement of Arf6 on spine formation and stability, although with somewhat contradictory conclusions. The finding in the present study that activators of Arf6 are specifically concentrated at the PSD opens the way for the unraveling of new mechanisms for the modification of spine morphology and function.

Acknowledgments—We thank Drs. T. S. Reese and J. Kowalak for advice and helpful discussions throughout this study.

* This work was supported in part by the Intramural Research Programs of the NINDS, National Institutes of Health and the National Institute of Mental Health. The costs of publication of this article were defrayed in part by the payment of page charges. This article must therefore be hereby marked “advertisement” in accordance with 18 U.S.C. Section 1734 solely to indicate this fact.

□ The on-line version of this article (available at <http://www.mcponline.org>) contains supplemental material.

¶ To whom correspondence should be addressed. Tel.: 301-496-4022; Fax: 301-451-5780; E-mail: markeys@mail.nih.gov.

REFERENCES

- Chen, X., Vinade, L., Leapman, R. D., Petersen, J. D., Nakagawa, T., Phillips, T. M., Sheng, M., and Reese, T. S. (2005) Mass of the postsynaptic density and enumeration of three key molecules. *Proc. Natl. Acad. Sci. U. S. A.* **102**, 11551–11556
- Cohen, R. S., Blomberg, F., Berzins, K., and Siekevitz, P. (1977) The structure of postsynaptic densities isolated from dog cerebral cortex. I. Overall morphology and protein composition. *J. Cell Biol.* **74**, 181–203
- Matus, A. I., and Taff-Jones, D. H. (1978) Morphology and molecular composition of isolated postsynaptic junctional structures. *Proc. R. Soc. Lond. B Biol. Sci.* **203**, 135–151
- Walsh, M. J., and Kuruc, N. (1992) The postsynaptic density: constituent and associated proteins characterized by electrophoresis, immunoblotting, and peptide sequencing. *J. Neurochem.* **59**, 667–678
- Walikonis, R. S., Jensen, O. N., Mann, M., Provance, D. W. J., Mercer, J. A., and Kennedy, M. B. (2000) Identification of proteins in the postsynaptic density fraction by mass spectrometry. *J. Neurosci.* **20**, 4069–4080
- Jordan, B. A., Fernholz, B. D., Boussac, M., Xu, C., Grigorean, G., Ziff, E. B., and Neubert, T. A. (2004) Identification and verification of novel rodent postsynaptic density proteins. *Mol. Cell. Proteomics* **3**, 857–871
- Li, K. W., Hornshaw, M. P., Van Der Schors, R. C., Watson, R., Tate, S., Casetta, B., Jimenez, C. R., Gouwenberg, Y., Gundelfinger, E. D., Smalla, K. H., and Smit, A. B. (2004) Proteomics analysis of rat brain postsynaptic density. Implications of the diverse protein functional groups for the integration of synaptic physiology. *J. Biol. Chem.* **279**, 987–1002
- Yoshimura, Y., Yamauchi, Y., Shinkawa, T., Taoka, M., Donai, H., Takahashi, N., Isobe, T., and Yamauchi, T. (2004) Molecular constituents of the postsynaptic density fraction revealed by proteomic analysis using multidimensional liquid chromatography-tandem mass spectrometry. *J. Neurochem.* **88**, 759–768
- Peng, J., Kim, M. J., Cheng, D., Duong, D. M., Gygi, S. P., and Sheng, M. (2004) Semiquantitative proteomic analysis of rat forebrain postsynaptic density fractions by mass spectrometry. *J. Biol. Chem.* **279**, 21003–21011
- Li, K., Hornshaw, M. P., van Minnen, J., Smalla, K. H., Gundelfinger, E. D., and Smit, A. B. (2005) Organelle proteomics of rat synaptic proteins: correlation-profiling by isotope-coded affinity tagging in conjunction with liquid chromatography-tandem mass spectrometry to reveal post-synaptic density specific proteins. *J. Proteome Res.* **4**, 725–733
- Collins, M. O., Yu, L., Coba, M. P., Husi, H., Campuzano, I., Blackstock, W. P., Choudhary, J. S., and Grant, S. G. (2005) Proteomic analysis of *in vivo* phosphorylated synaptic proteins. *J. Biol. Chem.* **280**, 5972–5982
- Trinidad, J. C., Thalhammer, A., Specht, C. G., Schoepfer, R., and Burlingame, A. L. (2005) Phosphorylation state of postsynaptic density proteins. *J. Neurochem.* **92**, 1306–1316
- Trinidad, J. C., Specht, C. G., Thalhammer, A., Schoepfer, R., and Burlingame, A. L. (2006) Comprehensive identification of phosphorylation sites in postsynaptic density preparations. *Mol. Cell. Proteomics* **5**, 914–922
- Cheng, D., Hoogenraad, C. C., Rush, J., Ramm, E., Schlager, M. A., Duong, D. M., Xu, P., Wijayawardana, S. R., Hanfelt, J., Nakagawa, T., Sheng, M., and Peng, J. (2006) Relative and absolute quantification of postsynaptic density proteome isolated from rat forebrain and cerebellum. *Mol. Cell. Proteomics* **5**, 1158–1170
- Kim, E., and Sheng, M. (2004) PDZ domain proteins of synapses. *Nat. Rev. Neurosci.* **5**, 771–781
- Collins, M. O., Husi, H., Yu, L., Brandon, J. M., Anderson, C. N., Blackstock, W. P., Choudhary, J. S., and Grant, S. G. (2006) Molecular characterization and comparison of the components and multiprotein complexes in the postsynaptic proteome. *J. Neurochem.* **97**, Suppl. 1, 16–23
- Satoh, K., Takeuchi, M., Oda, Y., Deguchi-Tawarada, M., Sakamoto, Y., Matsubara, K., Nagasu, T., and Takai, Y. (2002) Identification of activity-regulated proteins in the postsynaptic density fraction. *Genes Cells* **7**, 187–197
- Carlin, R. K., Grab, D. J., Cohen, R. S., and Siekevitz, P. (1980) Isolation and characterization of postsynaptic densities from various brain regions: enrichment of different types of postsynaptic densities. *J. Cell Biol.* **86**, 831–845
- Dosemeci, A., Reese, T. S., Petersen, J., and Tao-Cheng, J. H. (2000) A novel particulate form of Ca²⁺/calmodulin-dependent [correction of Ca²⁺/CaMKII-dependent] protein kinase II in neurons. *J. Neurosci.* **20**, 3076–3084
- Vinade, L., Chang, M., Schlieff, M. L., Petersen, J. D., Reese, T. S., Tao-Cheng, J. H., and Dosemeci, A. (2003) Affinity purification of PSD-95-containing postsynaptic complexes. *J. Neurochem.* **87**, 1255–1261
- Cho, K. O., Hunt, C. A., and Kennedy, M. B. (1992) The rat brain postsynaptic density fraction contains a homolog of the *Drosophila* discs-large tumor suppressor protein. *Neuron* **9**, 929–942
- Husi, H., Ward, M. A., Choudhary, J. S., Blackstock, W. P., and Grant, S. G. (2000) Proteomic analysis of NMDA receptor-adhesion protein signaling complexes. *Nat. Neurosci.* **3**, 661–669
- Husi, H., and Grant, S. G. (2001) Isolation of 2000-kDa complexes of N-methyl-D-aspartate receptor and postsynaptic density 95 from mouse brain. *J. Neurochem.* **77**, 281–291
- Masuda, J., Maynard, D. M., Nishimura, M., Ueda, T., Kowalak, J. A., and Markey, S. P. (2005) Fully automated micro- and nanoscale one- or two-dimensional high-performance liquid chromatography system for liquid chromatography-mass spectrometry compatible with non-volatile salts for ion exchange chromatography. *J. Chromatogr. A* **1063**, 57–69
- Yang, X., Dondeti, V., Dezube, R., Maynard, D. M., Geer, L. Y., Epstein, J., Chen, X., Markey, S. P., and Kowalak, J. A. (2004) DBParser: web-based software for shotgun proteomic data analyses. *J. Proteome Res.* **3**, 1002–1008
- Chelius, D., and Bondarenko, P. V. (2002) Quantitative profiling of proteins in complex mixtures using liquid chromatography and mass spectrometry. *J. Proteome Res.* **1**, 317–323
- Takamori, S., Holt, M., Stenius, K., Lemke, E. A., Grønborg, M., Riedel, D., Urlaub, H., Schenck, S., Brügger, B., Ringler, P., Müller, S. A., Rammner, B., Gräter, F., Hub, J. S., De Groot, B. L., Mieskes, G., Moriyama, Y., Klingauf, J., Grubmüller, H., Heuser, J., Wieland, F., and Jahn, R. (2006) Molecular anatomy of a trafficking organelle. *Cell* **127**, 831–846
- Morciano, M., Burre, J., Corvey, C., Karas, M., Zimmermann, H., and Volkandt, W. (2005) Immunoprecipitation of two synaptic vesicle pools from synaptosomes: a proteomics analysis. *J. Neurochem.* **95**, 1732–1745
- Wyszynski, M., Kharaznia, V., Shangvi, R., Rao, A., Beggs, A. H., Craig, A. M., Weinberg, R., and Sheng, M. (1998) Differential regional expression and ultrastructural localization of α -actinin-2, a putative NMDA receptor-anchoring protein, in rat brain. *J. Neurosci.* **18**, 1383–1392
- Petralia, R. S., Sans, N., Wang, Y. X., and Wenthold, R. J. (2005) Ontogeny of postsynaptic density proteins at glutamatergic synapses. *Mol. Cell. Neurosci.* **29**, 436–452
- Rubio, M. E., Curcio, C., Chauvet, N., and Bruses, J. L. (2005) Assembly of the N-cadherin complex during synapse formation involves uncoupling of p120-catenin and association with presenilin 1. *Mol. Cell. Neurosci.* **30**, 611–623
- Naisbitt, S., Kim, E., Tu, J. C., Xiao, B., Sala, C., Valtschanoff, J., Weinberg, R. J., Worley, P. F., and Sheng, M. (1999) Shank, a novel family of postsynaptic density proteins that binds to the NMDA receptor/PSD-95/GKAP complex and cortactin. *Neuron* **23**, 569–582
- Qiao, F., and Bowie, J. U. (2005) The many faces of SAM. *Sci. STKE* **2005**, re7
- Baron, M. K., Boeckers, T. M., Vaida, B., Faham, S., Gingery, M., Sawaya, M. R., Salyer, D., Gundelfinger, E. D., and Bowie, J. U. (2006) An architectural framework that may lie at the core of the postsynaptic density. *Science* **311**, 531–535
- Irie, M., Hata, Y., Takeuchi, M., Ichtchenko, K., Toyoda, A., Hirao, K., Takai, Y., Rosahl, T. W., and Sudhof, T. C. (1997) Binding of neuroligins to PSD-95. *Science* **277**, 1511–1515
- Lauren, J., Airaksinen, M. S., Saarma, M., and Timmusk, T. (2003) A novel gene family encoding leucine-rich repeat transmembrane proteins differentially expressed in the nervous system. *Genomics* **81**, 411–421
- Gulley, R. L., and Reese, T. S. (1981) Cytoskeletal organization at the postsynaptic complex. *J. Cell Biol.* **91**, 298–302
- van Rossum, D., and Hanisch, U. K. (1999) Cytoskeletal dynamics in dendritic spines: direct modulation by glutamate receptors? *Trends Neurosci.* **22**, 290–295
- Migaud, M., Charlesworth, P., Dempster, M., Webster, L. C., Watabe, A. M.,

- Makhinson, M., He, Y., Ramsay, M. F., Morris, R. G., Morrison, J. H., O'Dell, T. J., and Grant, S. G. (1998) Enhanced long-term potentiation and impaired learning in mice with mutant postsynaptic density-95 protein. *Nature* **396**, 433–439
40. El-Husseini, A. E., Schnell, E., Chetkovich, D. M., Nicoll, R. A., and Brecht, D. S. (2000) PSD-95 involvement in maturation of excitatory synapses. *Science* **290**, 1364–1368
 41. El-Husseini, A.-D., Schnell, E., Dakoji, S., Sweeney, N., Zhou, Q., Prange, O., Gauthier-Campbell, C., Aguilera-Moreno, A., Nicoll, R. A., and Brecht, D. S. (2002) Synaptic strength regulated by palmitate cycling on PSD-95. *Cell* **108**, 849–863
 42. Ehrlich, I., and Malinow, R. (2004) Postsynaptic density 95 controls AMPA receptor incorporation during long-term potentiation and experience-driven synaptic plasticity. *J. Neurosci.* **24**, 916–927
 43. Dakoji, S., Tomita, S., Karimzadegan, S., Nicoll, R. A., and Brecht, D. S. (2003) Interaction of transmembrane AMPA receptor regulatory proteins with multiple membrane associated guanylate kinases. *Neuropharmacology* **45**, 849–856
 44. Cottrell, J. R., Borok, E., Horvath, T. L., and Nedivi, E. (2004) CPG2: a brain- and synapse-specific protein that regulates the endocytosis of glutamate receptors. *Neuron* **44**, 677–690
 45. Dosemeci, A., Tao-Cheng, J. H., Vinade, L., Winters, C. A., Pozzo-Miller, L., and Reese, T. S. (2001) Glutamate-induced transient modification of the postsynaptic density. *Proc. Natl. Acad. Sci. U. S. A.* **98**, 10428–10432
 46. Dosemeci, A., Vinade, L., Winters, C. A., Reese, T. S., and Tao-Cheng, J. H. (2002) Inhibition of phosphatase activity prolongs NMDA-induced modification of the postsynaptic density. *J. Neurocytol.* **31**, 605–612
 47. Suzuki, T., Okumura-Noji, K., Tanaka, R., and Tada, T. (1994) Rapid translocation of cytosolic Ca²⁺/calmodulin-dependent protein kinase II into postsynaptic density after decapitation. *J. Neurochem.* **63**, 1529–1537
 48. Oh, J. S., Manzerra, P., and Kennedy, M. B. (2004) Regulation of the neuron-specific Ras GTPase-activating protein, synGAP, by Ca²⁺/calmodulin-dependent protein kinase II. *J. Biol. Chem.* **279**, 17980–17988
 49. Kim, J. H., Liao, D., Lau, L. F., and Huganir, R. L. (1998) SynGAP: a synaptic RasGAP that associates with the PSD-95/SAP90 protein family. *Neuron* **20**, 683–691
 50. Cox, R., Mason-Gamer, R. J., Jackson, C. L., and Segev, N. (2004) Phylogenetic analysis of Sec7-domain-containing Arf nucleotide exchangers. *Mol. Biol. Cell* **15**, 1487–1505
 51. Murphy, J. A., Jensen, O. N., and Walikonis, R. S. (2006) BRAG1, a Sec7 domain-containing protein, is a component of the postsynaptic density of excitatory synapses. *Brain Res.* **1120**, 35–45
 52. Someya, A., Sata, M., Takeda, K., Pacheco-Rodriguez, G., Ferrans, V. J., Moss, J., and Vaughan, M. (2001) ARF-GEP₁₀₀, a guanine nucleotide-exchange protein for ADP-ribosylation factor 6. *Proc. Natl. Acad. Sci. U. S. A.* **98**, 2413–2418
 53. Dunphy, J. L., Moravec, R., Ly, K., Lasell, T. K., Melancon, P., and Casanova, J. E. (2006) The Arf6 GEF GEP100/BRAG2 regulates cell adhesion by controlling endocytosis of beta1 integrins. *Curr. Biol.* **16**, 315–320
 54. Inaba, Y., Tian, Q. B., Okano, A., Zhang, J. P., Sakagami, H., Miyazawa, S., Li, W., Komiyama, A., Inokuchi, K., Kondo, H., and Suzuki, T. (2004) Brain-specific potential guanine nucleotide exchange factor for Arf, synArfGEF (Po), is localized to postsynaptic density. *J. Neurochem.* **89**, 1347–1357
 55. Shin, H. W., and Nakayama, K. (2004) Guanine nucleotide-exchange factors for arf GTPases: their diverse functions in membrane traffic. *J. Biochem. (Tokyo)* **136**, 761–767
 56. Donaldson, J. G., and Honda, A. (2005) Localization and function of Arf family GTPases. *Biochem. Soc. Trans.* **33**, 639–642
 57. D'Souza-Schorey, C., and Chavrier, P. (2006) ARF proteins: roles in membrane traffic and beyond. *Nat. Rev. Mol. Cell. Biol.* **7**, 347–358
 58. Miyazaki, H., Yamazaki, M., Watanabe, H., Maehama, T., Yokozeki, T., and Kanaho, Y. (2005) The small GTPase ADP-ribosylation factor 6 negatively regulates dendritic spine formation. *FEBS Lett.* **579**, 6834–6838
 59. Choi, S., Ko, J., Lee, J. R., Lee, H. W., Kim, K., Chung, H. S., Kim, H., and Kim, E. (2006) ARF6 and EFA6A regulate the development and maintenance of dendritic spines. *J. Neurosci.* **26**, 4811–4819